

Instability Thresholds And Generation of the Electron-Cloud in the GLC/NLC And Tesla Damping Rings

M. T. F. Pivi and T. O. Raubenheimer

Presented at Presented at the 9th European Particle Accelerator Conference
(EPAC 2004), 7/5/2004—7/9/2004, Lucerne, Switzerland

Stanford Linear Accelerator Center, Stanford University, Stanford, CA 94309

Work supported by Department of Energy contract DE-AC02-76SF00515.

INSTABILITY THRESHOLDS AND GENERATION OF THE ELECTRON CLOUD IN THE GLC/NLC AND TESLA DAMPING RINGS*

M. T.F. Pivi[†] and T. O. Raubenheimer SLAC, Menlo Park, CA 94025, USA

Abstract

In the beam pipe of the Damping Ring (DR) of a linear collider, an electron cloud may be produced by ionization of residual gas or photoelectrons and develop by the secondary emission process [1]. Coupling between the electrons and the circulating beam can cause coupled-bunch instabilities, coherent single-bunch instabilities or incoherent tune spreads that may lead to increased emittance, beam blow-up and ultimately to beam losses. We present recent computer simulation results for the electron cloud instability thresholds in the GLC/NLC (X-Band) main DR and for the TESLA DR.

INTRODUCTION

The electron cloud was identified as a possible limitation in the damping rings of a future linear collider in the ILC TRC document [2]. Extensive studies on the possible electron cloud effect have been performed at SLAC for the GLC/NLC and the TESLA positron main DR [3, 4, 5] and the positron low emittance transport lines. The results are obtained by computer simulation codes HEAD-TAIL, QUICKPIC, PEHTS (single-bunch), CLOUD_MAD (incoherent effects) and POSINST (coupled-bunch) [6, 7, 8, 9, 10] developed to study the electron cloud effect in particle accelerators. If the cloud is not suppressed, it will grow until it reaches an equilibrium density close to the neutralization level, ratio $e/p=1$, but in most cases the beam-cloud interaction sets a much lower limit on the acceptable cloud density. In this paper we will present the electron cloud density thresholds for the above mentioned effects. The generation and development of the electron cloud in the linear collider damping rings is discussed in [11].

HEAD-TAIL AND SINGLE-BUNCH INSTABILITY

We have estimated the electron cloud density threshold for the single-bunch fast head-tail instability in the X-band and TESLA damping rings. The results have been benchmarked with three different simulation codes, namely HEAD-TAIL [7], QUICKPIC [9] and PEHTS [10]. The interaction between the electrons and the beam particles is expressed by the equation of motion

$$\frac{d\mathbf{p}_p}{ds} = -\frac{2r_e}{\gamma} \frac{\partial \phi_e(\mathbf{r})}{\partial \mathbf{r}} \quad \frac{d\mathbf{p}_e}{dt} = -2r_e c \frac{\partial \phi_p(\mathbf{r})}{\partial \mathbf{r}} \quad (1)$$

where r_e is the classical electron radius, $\mathbf{p}_{p,e}$ respectively the beam particle and the electron momentum and $\phi_{e,p}$ are

Table 1: Simulation parameters for the GLC/NLC or X-band and the TESLA positron damping rings.

Parameter	Symbol	X-Band	TESLA
Ring circumference	C , m	299.8	17000
Bunch population	$N_p \times 10^{10}$	0.75	2
Beta funct. kick sec.	β_x, β_y m	10, 10	35, 65.7
Bunch length	σ_z , mm	5.5	6.0
Tr. rms bunch size	σ_x, σ_y μ m	49, 6	103, 7.3
Long. mom. spread	Δp	9.7e-4	1.3e-3
Mom. compaction	α	1.33e-3	1.22e-4
Synchrotron tune	ν_z	0.0118	6.59e-2
Horizontal tune	ν_x	21.150	76.31
Vertical tune	ν_y	10.347	41.18
Chromaticity	ξ_x, ξ_y	correct.	correct.

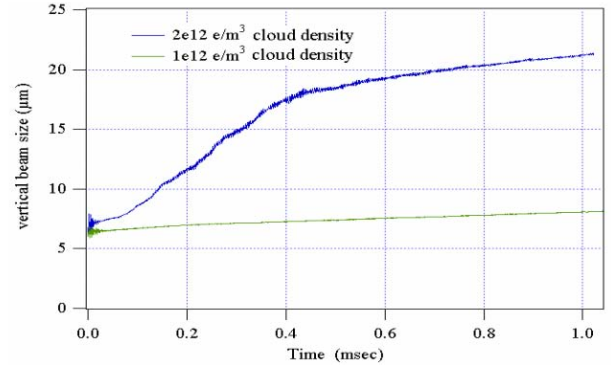


Figure 1: Simulation of single-bunch beam instability from electron cloud in GLC/NLC Damping Ring.

the electron cloud and the beam potentials. The typical number of kicks received by the bunch per turn is typically varying between 1 and 10. A discrete Fast Fourier Transform (FFT) in two dimensional space and a particle-in-cell (PIC) algorithm are used to compute the potential. The electrons oscillate in the linearized beam potential with an angular frequency ω

$$\omega_{c,y}^2 = \frac{2\lambda_b r_e c^2}{(\sigma_x + \sigma_y)\sigma_y} \quad (2)$$

where λ_b is the beam line density and $\sigma_{x,y}$ the transverse beam size. Due to the electron cloud oscillation and pinching the cloud density increases along the bunch. An electron cloud wakefield is established which drives the oscillations of the tail of the bunch. The interchange of the head with the tail by synchrotron oscillations is a damping mech-

*Work supported by the US DOE under contracts DE-AC03-76SF00515 and DE-AC03-76SF00098.

[†] mpivi@slac.stanford.edu

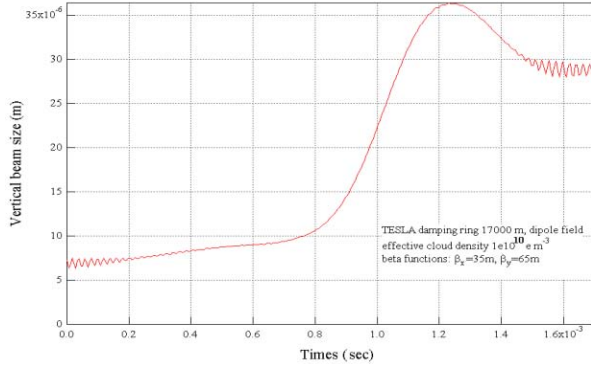


Figure 2: Simulation of single-bunch instability from electron cloud in the 17000 m long TESLA DR using HEAD-TAIL.

anism for the fast head-tail effect. Thus, the maximum allowed electron cloud density depends on the synchrotron tune and the driving force. In the X-band MDR, an head-tail instability is observed to occur for an average electron cloud density close to $2.0 \times 10^{12} \text{ e m}^{-3}$, as shown in Fig. 1, with growth time on the order of $100 \mu\text{sec}$. The three codes show consistent results. This is one order-of-magnitude lower than the expected cloud neutralization level if a cloud is allowed to form as shown in Table 2. A slightly positive chromaticity or a larger synchrotron tune increases the instability threshold as expected, but this is unlikely to provide the margin of safety that is desired. The single-bunch instability threshold for the 17000 m long TESLA DR is at $1.0 \div 5.0 \times 10^{10} \text{ e m}^{-3}$ also well below the expected cloud neutralization level, see Figs 2; TESLA DR simulation results have been benchmarked against the three codes and are consistent, see Fig. 3. Furthermore, the instability is accompanied by severe beam particle losses in the first few turns. Finally, we have used CLOUD_MAD to compute the possible incoherent tune spread along the bunch when passing through the TESLA wiggler beam line with result shown in Fig. 4. A summary of the Electron cloud instability thresholds for both damping rings are listed in Table 2.

Table 2: Electron cloud density thresholds in units of (e m^{-3}) for incoherent tune spread, single- (SB) and coupled- (MB) bunch instability. The average neutralization level is also shown.

Parameter	X-Band MDR	TESLA DR
Av.neutralization	$2.0 \times 10^{13} \text{ e m}^{-3}$	$8.0 \times 10^{11} \text{ e m}^{-3}$
$\Delta\nu = 0.05$	$1.6 \times 10^{12} \text{ e m}^{-3}$	$2.3 \times 10^{10} \text{ e m}^{-3}$
Single-Bunch	$2.0 \times 10^{12} \text{ e m}^{-3}$	$1.0 \times 10^{10} \text{ e m}^{-3}$
Coupled-Bunch	$3.0 \times 10^{13} \text{ e m}^{-3}$	$1.6 \times 10^{13} \text{ e m}^{-3}$

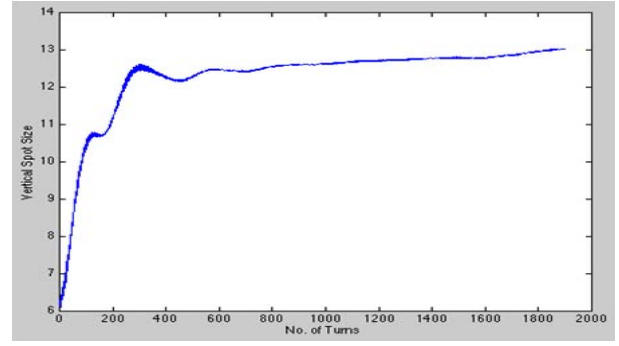


Figure 3: Simulation of single-bunch instability from electron cloud in the TESLA DR using QUICKPIC code, for a cloud density of $1 \text{e} 10 \text{ e m}^{-3}$.

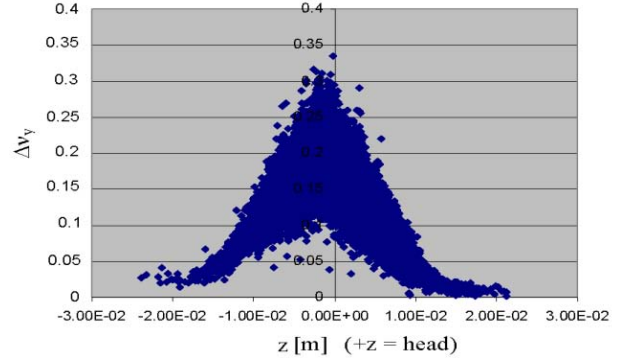


Figure 4: Vertical tune shift after passing through the TESLA wiggler beam line which has 432 meters of wiggler in 520 meters of beam line. An electron cloud density of $6 \text{e} 12 \text{ e m}^{-3}$ is assumed. No magnetic field was included.

COUPLED-BUNCH INSTABILITY

The calculation of the coupled-bunch wake field is implemented in the POSINST code. After an electron-cloud have reached an equilibrium density a single perturbing bunch is displaced from the central orbit by Δy . The electron cloud is perturbed dynamically causing a dipole wake which affects the subsequent bunches. Simulation results show that the wake is significant for few trailing bunches following the perturbing bunch. Thus, with good approximation, the instability growth rate τ_0^{-1} is given by the first $k=1$ collective oscillation mode term as

$$\tau_0^{-1} = \frac{ce^2 N_p}{4\pi E \nu_{\beta,y}} |W(s_B)| \quad (3)$$

where E is the beam energy, s_B the bunch spacing from the displaced bunch and $\nu_{\beta,y}$ the vertical betatron tune. We use to define the coupled-bunch instability threshold as the cloud density that results in a $\sim 100 \mu\text{sec}$ growth time, which can be conveniently corrected by the feedback system. Thus, in the X-band main damping ring the threshold is computed at a cloud density $> 3.0 \times 10^{13} \text{ e m}^{-3}$, see Fig. 5. Similarly, the threshold in the TESLA DR is at cloud density $> 1.6 \times 10^{13} \text{ e m}^{-3}$.

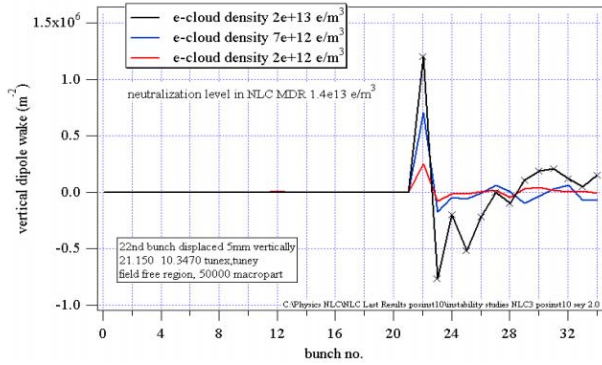


Figure 5: Long range wake field in the X-Band DR.

R&D EFFORT TO REDUCE THE SEY

The electron cloud develops under conditions where the average secondary electron yield (SEY) of the electrons hitting the beam pipe wall is larger than one. SLAC has an active R&D effort to find a cure for the electron cloud effect by proper surface treatments. In particular, we are measuring the SEY of thin film coatings, exploring durability and conditioning strategies, investigating new surface grooved profile design and finally planning to install test demonstration chambers in PEP-II. We have recently developed metal surfaces with triangular and rectangular grooved design profile. Such a surface is expected to reduce the escape probability of secondary emitted electrons, reducing considerably the effective SEY [12, 13]. A fabricated aluminum triangular surface design with an opening 40 degree angle shows a SEY reduction of 35%. We measured a peak SEY of ~ 0.75 for the rectangular copper sample profile shown in Fig 6. A test chamber with a grooved profile is planned to be installed in PEP-II.

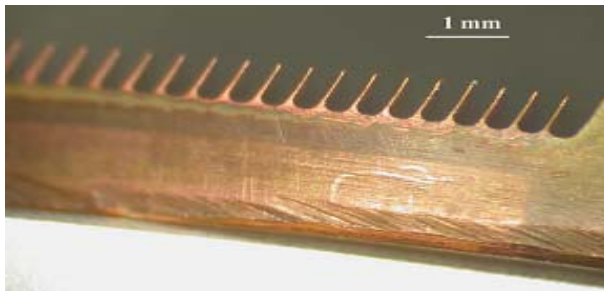


Figure 6: Rectangular groove surface profile: 0.8mm depth, 0.35mm step and 0.05mm rect. groove thickness.

CONCLUSIONS

We have estimated the threshold instability for the electron cloud density for the X-Band and TESLA linear collider damping rings. A promising possible solution is the use of rectangular grooves surface profile that would reduce the SEY of the vacuum chamber below 0.8 and lower.

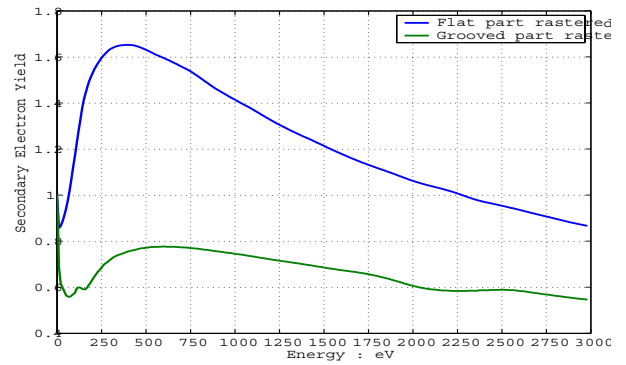


Figure 7: Measurements of the flat part of a Cu sample (top curve) and for the rectangular groove surface part (bottom curve). A peak secondary yield as low as 0.75 has been measured.

We are particularly grateful to K. Ohmi, A. Z. Ghalam, F. Zimmermann, G. Rumolo, E. Benedetto and R. Wanzenberg for simulation related discussion and studies, and to R. Kirby and Le Pimpec and G. Stupakov.

REFERENCES

- [1] For updates on electron cloud studies, see Proc. ICFA ECLLOUD04 Workshop, 2004: <http://icfa-ecloud04.web.cern.ch/icfa-ecloud04/>. In particular contributions by R. Wanzenberg, M. Pivi and F. Zimmermann.
- [2] ILC-TRC Report 2003: <http://www.slac.stanford.edu/xorg/ilc-trc/2002/2002/reports/03rep.htm>.
- [3] A. Woslki and M. Woodley, SLAC NLC LCC-0113, 2003.
- [4] R. Brinkmann, K. Flöttmann, J. Roßbach, P. Schmüser, N. Walker, H. Weise *TESLA Technical design Report* (2001).
- [5] M. Pivi, T. O. Raubenheimer and M. A. Furman in the Proc. PAC2003 Conf.
- [6] M. A. Furman and G. R. Lambertson, LBNL-41123/CBP Note-246, 1997.
- [7] G. Rumolo and F. Zimmermann *Phys. Rev. STAB*, Vol. 5, 121002 (2002).
- [8] CLOUD_MAD, T. Raubenheimer; reference page http://www-project.slac.stanford.edu/lc/local/AccelPhysics/Codes/Ion_MAD-Cloud_Mad/dbates/nlc_cloudmadtools.doc/cloud_mad/index.html
- [9] T. Katsouleas, A. Z. Ghalam, S. Lee, W. B. Mori, C. Huang, V. Decyk and C. Ren CERN Yellow Report No. CERN-2002-001, p. 239.
- [10] K. Ohmi in Proc. PAC 2001 Conf.
- [11] M. Pivi, for publication in *Phys. Rev. STAB*, special collection ECLLOUD04 Workshop.
- [12] A. Krasnov CERN LHC Project Report 671.
- [13] G. Stupakov and M. Pivi in [1]